

Precision Length Measurements by Multi-Wavelength Interferometry

R. Schödel, K. Meiners-Hagen, F. Pollinger, A. Abou-Zeid

Physikalisch-Technische Bundesanstalt (PTB), Bundesallee 100,
D-38116 Braunschweig, Germany
Email: Ahmed.Abou-Zeid@ptb.de

Abstract. *Three different applications of multi-wavelength interferometry are reviewed which have been developed at PTB. They demonstrate the high precision achievable by this technique on multiple scales, from absolute geodetic distances up to 10 m, over prismatic bodies, e.g. gauge blocks, in the sub-meter regime, down to the microscopic roughness of surfaces.*

Keywords: interferometry, diode laser, length measurement, long distance, surface profile, gauge blocks

1. Introduction

Displacement measurements by a laser interferometer are typically performed by moving one reflector of the interferometer along a guideway and counting the periodic interferometer signal, e.g. the interference fringes. Such a counting technique requires a relatively slow continuous movement of the reflector along the entire distance to be measured. When the integer order of interference is lost during the movement, only the fractional order of interference is obtained (phase/ 2π) resulting in a length unambiguity of $\lambda/2$, only. This small unambiguity can be enlarged by using more than one wavelength, i.e. multi-wavelength interferometry.

An ambiguity of lengths measured by single-wavelength interferometry also occurs when there are length discontinuities at the surfaces of objects to be measured resulting in phase steps. Using two wavelengths $\lambda_{1,2}$, the difference of two interferometer phases acts like a single phase of a "synthetic" wavelength $\Lambda = \lambda_1 \cdot \lambda_2 / (\lambda_1 - \lambda_2)$ which is longer than both optical wavelengths. Within half of this synthetic wavelength no counting of interference fringes is necessary. The measurement uncertainty, however, is increased if the measured length L is calculated using the synthetic wavelength. Each uncertainty in both, phase measurements and in the wavelengths is scaled by the ratio of synthetic to optical wavelength. To overcome this problem, it is effective to use the synthetic wavelength only for calculation of the fringe order of the optical wavelengths and benefit from the lower uncertainty of the latter for the length measurement. In this case the measurement uncertainty with the synthetic wavelength must not exceed one quarter of the optical wavelengths to get their correct fringe order. The maximum possible synthetic wavelength is therefore limited. To get a larger range of unambiguity more wavelengths can be used which offer different synthetic wavelengths. Starting from the longest one, each synthetic wavelength is used to get the fringe order of the next shorter one and finally that of an optical wavelength.

In general, multiple lasers are necessary for the multi-wavelength technique whose beams have to be aligned on the same path of the interferometer. These must be detected simultaneously after their separation at the interferometer output for avoiding errors due to the thermal and mechanical drift of the setup.

The effort can be reduced by using wavelength tunable diode lasers. The specific features of such lasers are their tunability by variation of the injection current and the availability of

wavelengths from infrared to blue light. This offers a wide range of possible synthetic wavelengths. Depending on the application, the frequency of diode lasers has to be stabilised. By simple parameter stabilisation, i.e. injection current and heat sink temperature, the vacuum wavelength variation is of the order of $\Delta\lambda/\lambda > 10^{-7}$ within days and up to 10^{-5} long term [1]. More sophisticated methods like stabilising the laser on an external cavity or onto atomic or molecular absorption lines, e.g. rubidium, potassium, or iodine, improves the stability by orders of magnitude ($< 10^{-9}$) [2], [3].

This paper gives an overview of three different applications of multi-wavelength interferometry which are well established at PTB: precise measurements of absolute distances (Chap. 2), surface profiles (Chap. 3) and length of prismatic bodies (Chap. 4).

2. Precise measurements of absolute distances

The measurement of distances in the order of ten metres with a relative measurement uncertainty of 10^{-6} is important in a variety of practical applications such as the positioning of components in automotive engineering or aircraft construction, or the inspection of windmill blades. Optical measurements of such distances are typically performed by laser trackers. Recent laser trackers are based on two different length measurement methods: a standard counting interferometer with a HeNe laser and an absolute distance measuring system using a time of flight measurement with an amplitude modulated diode laser. The uncertainty of the absolute length measurement is larger than some 10 μm . Conventional counting interferometers provide a smaller uncertainty but require that the beam follows the reflector movement so that the interference fringes can be counted continuously. In practice, this requires increased efforts and leads to a considerable increase of measurement time. Under well controlled ambient conditions relative measurement uncertainties of 10^{-7} can be achieved.

Absolute distance interferometers (ADI) [4]-[7] achieve a better resolution than systems measuring the time of flight. They could meet the above demand concerning a relative measurement uncertainty of 10^{-6} . Nevertheless, they are not widely used in practice till now, probably due to the complexity of their implementation. Here, an approach to an ADI based on a homodyne interferometer with two diode lasers is presented.

Absolute distance interferometry with a variable synthetic wavelength is performed by use of a laser whose emission frequency ν can be tuned continuously. Diode lasers, with a large mode-hop free tuning range for this purpose, are usually used. In the case of an external cavity diode laser the tuning of the laser frequency $\Delta\nu$ (typically 50...100 GHz) is obtained by changing the diffraction angle by tilting the grating (Littrow type) or by tilting the mirror (Littman type) in the external resonator. In case of a distributed feedback laser diode (DFB) the injection current is modulated. The laser frequency is usually tuned periodically by an oscillator.

In an interferometer the phase Φ is generally given by

$$\Phi = \frac{4\pi}{\lambda_0} nL = \frac{4\pi\nu}{c} nL . \quad (1)$$

Here, λ_0 is the laser wavelength in vacuum, ν the laser frequency, c is the velocity of light in vacuum, L is the arm length difference in the interferometer, and n is the refractive index of air. The latter requires the measurement of the ambient parameters (temperature, air pressure, humidity) and can be derived from an Edlén-type empirical equation [8].

In an absolute interferometer the length L_{ADI} , i.e. the length difference between the two interferometer arms, can be calculated from the phase change $\Delta\Phi$ caused by the frequency tuning $\Delta\nu$ according to

$$L_{ADI} = \frac{c}{4\pi n} \frac{\Delta\Phi}{\Delta\nu}. \quad (2)$$

In this case $\Delta\nu$ may be obtained from the transmission of a Fabry-Pérot resonator. The laser frequency at the transmission peaks is given by $\nu = \nu_0 + i \cdot FSR$, with FSR being the free spectral range of the resonator, i the number of the transmission peaks which are swept during the tuning, and ν_0 the initial frequency. Thus, the factor $\Delta\Phi/\Delta\nu$ in (2) is obtained as the slope of a linear interpolation of the phases $\Delta\Phi(i)$.

Alternatively, the light of the laser can be coupled simultaneously into the ADI and into a reference interferometer of a known length L_{ref} which has to be determined independently. The length L_{ADI} of the ADI can be calculated from the phase changes in the ADI ($\Delta\Phi_{ADI}$) and in the reference interferometer ($\Delta\Phi_{ref}$):

$$L_{ADI} = L_{ref} \frac{n_{ref}}{n_{ADI}} \frac{\Delta\Phi_{ADI}}{\Delta\Phi_{ref}}. \quad (3)$$

The refractive indices have to be considered in the ADI (n_{ADI}) and in the reference interferometer (n_{ref}). If both interferometers are placed closely together, the refractive indices are almost equal, and their influence almost cancels out. During the tuning of the laser frequency several phase values from both interferometers are recorded and then fitted to a linear function which passes the origin. The number of data pairs for the fit is only limited by the measurement rate (speed of the detector electronics and A/D conversion). This is a significant advantage compared to the use of a Fabry-Pérot resonator as reference because in the latter case only a limited number of transmission peaks can be used for data sampling.

Length changes, due to, e.g., reflector vibrations that occur during the tuning of the laser frequency, contribute considerably to the measurement uncertainty of frequency sweeping interferometry. If the length is not constant in time, the measured phase values $\Delta\Phi_{ADI}$ in (2) and (3) correspond to different values of L_{ADI} . Variations of L_{ADI} are scaled up with the ratio $\nu/\Delta\nu$, which is typically in the range of 10^3 to 10^4 . In the case of vibrations, the impact on L_{ADI} can be reduced by averaging over an appropriate number of single measurements.

In our approach to absolute distance interferometry, we monitor changes of the length L_{ADI} during tuning by a conventional counting interferometer with a permanently frequency stabilised laser with the vacuum wavelength λ_1 , which runs parallel to the ADI. The phase change $\Delta\Phi_{ADI}$ of the ADI originating from frequency tuning is corrected by the result of the stabilised laser:

$$\Delta\Phi_{ADI} (corr.) = \Delta\Phi_{ADI} - \frac{\lambda_1 n_2}{\lambda_2 n_1} \Delta\Phi_1. \quad (4)$$

Here, $\Delta\Phi_1$ is the measured phase change of the conventional interferometer. n_1 and n_2 are the refractive indices for λ_1 and λ_2 in the ADI. They differ from each other only due to the dispersion in air since both beams are on the same optical path. The central vacuum wavelength of the tuned laser is denoted as λ_2 . By inserting (4) into (3), the final result L_{ADI} for the coarse measurement is obtained.

The range of unambiguity can be extended by using more than one wavelength in the

interferometer. If the interferometer is operated with two optical wavelengths λ_1 and λ_2 the difference $\Delta\Phi_{synth}$ between the phases is given by

$$\Delta\Phi_{synth} = \Phi_2 - \Phi_1 = \left(\frac{4\pi}{\lambda_2} - \frac{4\pi}{\lambda_1} \right) nL = \frac{4\pi}{\Lambda} nL ,$$

$$\Lambda = \frac{\lambda_1 \lambda_2}{\lambda_2 - \lambda_1} . \quad (5)$$

The phase difference $\Delta\Phi_{synth}$ corresponds to the phase of a fixed synthetic wavelength Λ . It is larger than the optical wavelengths and determines the range of unambiguosness to $\Lambda/2$. Here the wavelengths are assumed to be closely together so that the refractive index n is approximately identical for both wavelengths. By considering not only the phase difference, but the phases itself the range of unambiguosness can be extended to more than $\Lambda/2$. After moving the reflector by one period of the synthetic wavelength the phase difference $\Delta\Phi_{synth}$ is the same as before, but the single phase values are usually different after the movement. When the phase measurement itself has a low uncertainty, a “phase recovery criterion” can be applied. In principle such criterion corresponds to the “method of exact fractions” as further discussed in Chap. 4.

If several synthetic wavelength are used, the longest one determines the unambiguous measuring range. The measurement uncertainty increases according to the ratio of the synthetic to the optical wavelengths. Therefore, the shortest synthetic wavelength gives the lowest uncertainty. The length result from one synthetic wavelength is typically used to determine the fringe order of the next shorter synthetic wavelength.

Since the absolute distance interferometry with a variable synthetic wavelength uses a frequency stabilised laser 1 and a second frequency swept laser 2, it seems straightforward to expand this setup for a measurement with a fixed synthetic wavelength. For that purpose the frequency sweep from laser 2 has to be stopped, and the laser has to be stabilised. The measurement consists of two steps: First, the integer order of interference for Λ is determined by the measurement with variable synthetic wavelength according to (3) and (4). After switching the modulated laser in the stabilised mode, the fractional order of interference is determined according to (5). Thus, the final result L of the two-stage length measurement is

$$L = \left\lfloor \frac{L_{ADI}}{\Lambda/2} - \frac{\Delta\Phi_{synth}}{2\pi} + \frac{1}{2} \right\rfloor \frac{\Lambda}{2} + \frac{\Delta\Phi_{synth}}{2\pi m} \frac{\Lambda}{2} , \quad (6)$$

where $\lfloor x \rfloor$ denotes the floor function which returns the largest integer $\leq x$. The synthetic phase $\Delta\Phi_{synth}$ is measured without counting fringes and is in the range $\Delta\Phi_{synth} \in [0 \dots 2\pi]$. The subtraction of the term with $\Delta\Phi_{synth}$ and the addition of $1/2$ in the floor function has a practical reason: without these terms the equation is mathematically correct, but the measurement uncertainties lead to a scatter of L_{ADI} . At the border between two fringe orders even a small scatter can lead to the wrong fringe order. Both terms shift the value in the floor function mathematically to constant levels of $1/2, 3/2, 5/2, \dots$, which lead to the fringe order $0, 1, 2, \dots$. Therefore, scatter smaller than $\Lambda/4$ has no influence on determining the fringe order. It should be noted that this absolute interferometer can also be applied as laser tracker, i.e. as a standard counting interferometer using the permanently stabilised laser.

The optical setup of our ADI as a homodyne Michelson interferometer is depicted in Fig. 1. Laser 1 is a Littrow type extended cavity diode laser (ECDL) operating at approx. 770.1 nm

wavelength, and laser 2 is a Littman type ECDL at approx. 766.7 nm wavelength. Both lasers are equipped with antireflection coated laser diodes. For both ECDLs, a small amount of their intensity is split off by a combination of a half-wave plate and a polarizing beam splitter and is fed to a setup using polarization-optical differential detection for the stabilisation to Doppler-reduced potassium (K) absorption lines as described for Rubidium in [2]. Laser 1 is permanently stabilised to a K-D1 line. The emission frequency of laser 2 is tuned by the use of a programmable function generator. A low pass filtered and smoothed triangle signal with a frequency of 5...10 Hz is used for the modulation.

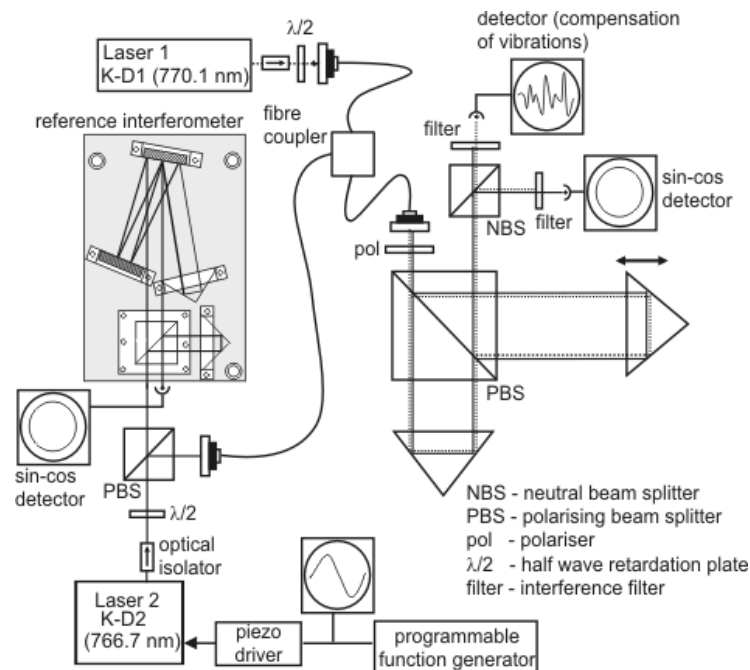


Fig. 1. Optical setup of the absolute distance interferometer with two ECDLs. The light of both diode lasers is coupled into a Michelson interferometer via one polarization maintaining single mode fibre. For clarity, the details for the stabilisation of the ECDLs to potassium absorption lines are not shown.

A portion of the modulated laser's intensity is coupled into the reference interferometer which is placed in a temperature stabilised box. For the ADI, both laser beams are coupled into one polarisation maintaining single mode fibre in order to ensure that they traverse the interferometer on identical paths. By the use of a half-wave plate in front of and a polarizer behind the fibre, matching of the polarization of the lasers light with the fibre axis is achieved. At the interferometer output the two beams are separated by a grating for detection. The interferometer is composed of a polarizing beam splitter and two triple reflectors.

The interference signals are processed within the detectors in such a manner that two signals are obtained which are shifted by 90° to each other. To obtain these quadrature signals for the modulated laser, it has turned out advantageous to use Fresnel rhombi instead of quarter wave plates since for the latter the retardation is more strongly dependent on the wavelength. The quadrature signals for the ADI, the reference interferometer, and the counting interferometer operated by laser 1 are recorded with an acquisition rate of $250000 \text{ samples s}^{-1}$ by a 16-bit, 8 channel A/D converter card. First, a data block is sampled with a length depending on the averaging time. The raw sine-cosine values are processed by a Heydemann correction [9]. Since the frequency modulated laser has a slight amplitude modulation the sine-cosine signals do not follow an ellipse but have a slightly spiral shape. The amplitude modulation is $\approx 5\%$ of

the total intensity so that for a few 2π periods an ellipse is a good approximation. Therefore several ellipse fits over a few periods instead of one over all data points are calculated.

Subsequently, single phase values are calculated by the arctan function, and are sorted according to the rising and falling edges of the modulation. The phase of the ADI is corrected by the phase of the stabilised laser interferometer according to (4). For each edge, the phases of the ADI and the reference interferometer are linearly interpolated by a least square fit with the axis intercept set to zero. With the slope, the length L_{ADI} is determined according to (3).

For the fixed synthetic wavelength approach, laser 2 is stabilised on a K-D2 absorption line at approx. 776.1 nm giving a synthetic wavelength of $\approx 173 \mu\text{m}$. The fractional part of the length can be directly evaluated from (6) after the Heydemann correction. In the case of stabilised lasers, it is sufficient to determine the parameters for the Heydemann correction during a slow movement of the measurement reflector prior to the measurement.

Length measurements with the setup shown in Fig. 1 were performed at the geodetic base of the PTB. It consists of a 50 m long bench with a moving carriage and is equipped with a conventional counting HeNe laser interferometer with a folded beam path, which was used as reference. The refractive index of air is determined by the Edlén equation [8]. The environmental parameters were measured by one air pressure and one relative humidity sensor, and temperature by PT100 sensors placed at an interval of 2.5 m along the bench. Results of measurements for lengths of ~ 2 m were published in [7].

The combined evaluation of ADI and fixed synthetic wavelength measurements of distances up to approximately 10 m leads to results shown in Fig. 2. According to the data, the deviation between the ADI and the HeNe interferometer is below $0,5 \mu\text{m} + 0,5 \mu\text{m}/\text{m}$ except of three points. Thus, the well known approach of an absolute interferometer with one laser with modulated laser frequency and a second, frequency stabilised laser for compensation of vibrations can be improved by frequency stabilising both lasers and using the synthetic wavelength for further interpolation of the result.

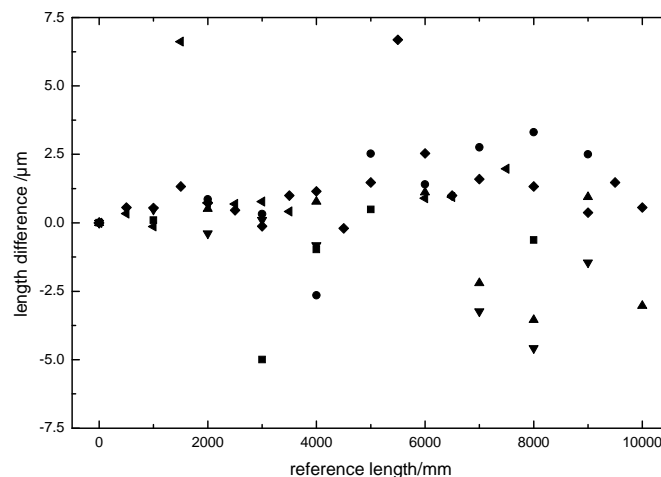


Fig. 2. Difference between the absolute interferometer and a counting HeNe laser interferometer as a function of the reference length after evaluation according to equation (6). The different symbols denote individual measurements.

3. Precise length measurements of surface profiles

High precision measurements of surface topography and properties like roughness are important tasks in quality assurance and control. There are a number of different technologies which differ by the measurement principle, operating complexity, resolution, and measuring range. Interferometric methods have a very high resolution within the nanometre range. Laser interferometers, however, are giving ambiguous results for distance variation of more than half the wavelength λ , e.g. due to steps in the surface. Nevertheless, using the multi-wavelength technique the interferometric measurement of surface profiles is possible.

For the measurement of surface profiles the measuring range of the interferometer was supposed to be in the order of 100 μm . Using parameter stabilised laser diodes three wavelengths were necessary. Wavelengths of 789.5 nm, 822.95 nm, and 825.3 nm were chosen which lead to synthetic wavelengths of approx. 14.0 μm , 14.8 μm , and 289 μm .

A modulation technique allows the separation of the wavelengths at the interferometer output. The injection current of the three laser diodes is modulated with different frequencies ω_m around 1 MHz. This results in a modulation of the laser frequency by $\Delta\nu$ and a modulation of the interferometer phase. At the interferometer output a spectrum appears with harmonics of ω_m . The amplitude of two adjacent harmonics are proportional to the sine and cosine of the interferometer phase. Lock-in amplifiers detecting at the second and third harmonic give a quadrature signal [10].

The different modulation frequencies of the laser diodes allow the simultaneous detection of the three interferometer signals with only one photo detector. The optical setup, sketched in Fig. 6, is also simplified by the modulation technique.

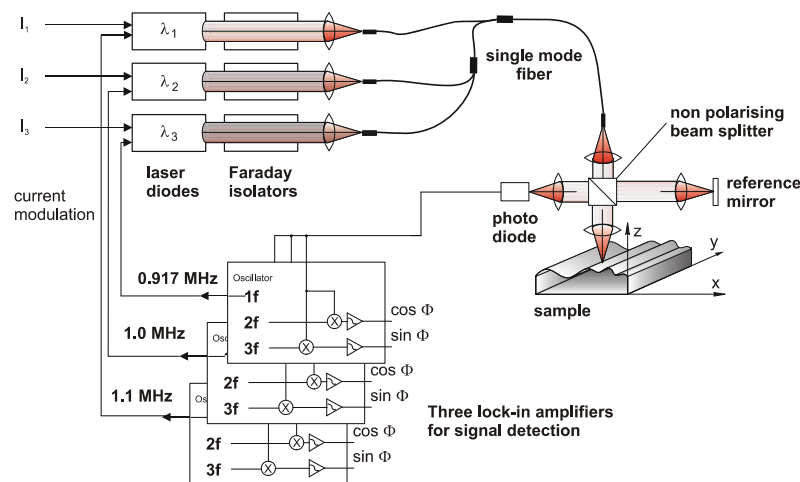


Fig. 6 Optical setup of the surface profilometer with a multiple wavelength diode laser interferometer

The beams of the diode laser are coupled into one single mode fibre. Faraday isolators protect the diodes from feedback light. The fibre is connected to a simple unbalanced Michelson interferometer without polarization optical components. One arm of the interferometer leads to the reference mirror, the light of the other arm is focused onto the sample. Depending on the measurement range in z-direction, i.e. focus depth, and on the lateral resolution, the focal length of the objective lens can be chosen suitable according to the surfaces under investigation. The sample can be moved in both lateral directions with mechanical translation stages by approximately 15 cm.

The developed diode laser profilometer was tested using a PTB depth setting standard chosen as a test surface with a well-known surface topography [11]. This standard is a glass block, 8 mm thick, 20 mm wide, and 40 mm long with six grooves of circular profile, the depth ranging from 190 nm to 9.2 μm . The reference values of this standard have been reproduced within the uncertainties stated for the depth setting standard as shown in table 1.

Table 1. Comparison of the measured groove depths with the reference values of a depth setting standard.

| Diode laser profilometer / nm | PTB reference value / nm |
|-------------------------------|--------------------------|
| 196 | 191 \pm 6 |
| 445 | 440 \pm 6 |
| 945 | 952 \pm 10 |
| 2130 | 2141 \pm 32 |
| 4520 | 4543 \pm 48 |
| 9225 | 9208 \pm 80 |

The measurement uncertainty of the profilometer is limited by the quality of the translation stages (~ 25 nm). The uncertainty of the interferometer itself is estimated to approximately 20 nm for a 100 μm measuring range and an arm length difference of 10 cm [10]. Moreover, uncertainty contributions arise from the long and short term wavelength stability of diode lasers used (1 nm and 10 nm, respectively). Contributions due to changes of the refractive index of air are negligible. A further uncertainty contribution can arise from the phase measuring, e.g. due to the lock-in amplifiers, or optical quality of the surface. This contribution amounts to approx. 4 nm for smooth, highly reflective surfaces.

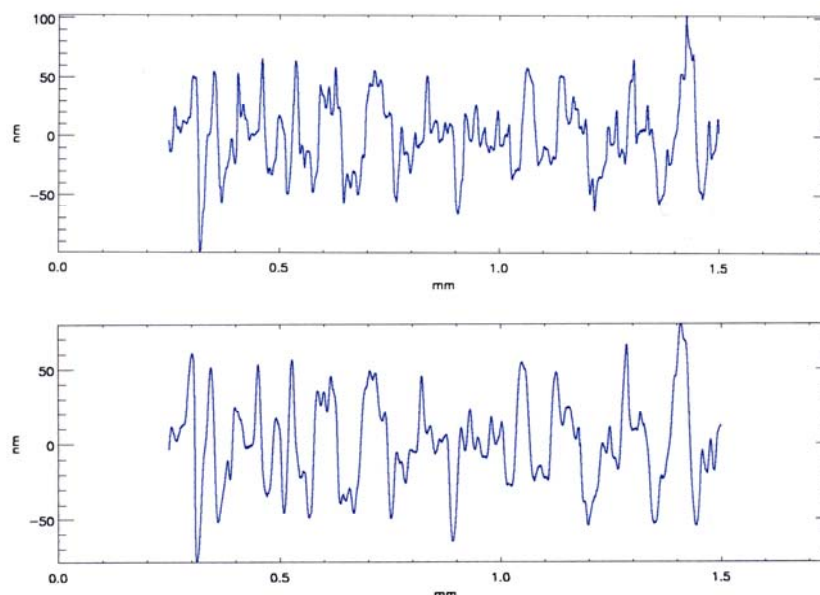


Fig. 4. Surface profile measured with a contact stylus instrument (upper curve) and with the interferometer (lower curve)

On rough surfaces the interference contrast varies over the sample which affects the interferometer signal. Three so-called “superfine roughness standards” with R_z values between 134 nm and 450 nm were measured to investigate the limits of the interferometer on

rough surfaces. These standards are cylindrical disks with approx. 50 mm diameter with a 4 mm wide rough zone around the centre. Figure 4 shows a part of the surface profile of a roughness standard with an average maximum height $R_z = 134$ nm as measured with the diode laser interferometer in comparison with the contact stylus instrument. It turns out that the profile is well reproduced by the interferometer. However, fine details like the sharp spike near position

1.4 mm and the narrow groove near 0.3 mm are smoothed by the interferometer. This is caused by the focus diameter of approx. $2 \mu\text{m}$ of the microscope objective used for these measurements so that the measured height values are averaged over this range. This smoothing leads to an apparent decrease of the roughness. All roughness parameters derived from the interferometer data are smaller than their reference values from the calibration with a contact stylus instrument. The roughness average R_a is well reproduced by the interferometer data. The maximum deviation to the reference value is 9%. The other averaged roughness parameters like rms roughness R_q which are not shown here have similar deviations. The average maximum height R_z and the maximum roughness depth R_{max} as peak values are up to 17% smaller than their reference values.

As shown above the use of the three-wavelength diode laser interferometer offers a measurement range of $\approx 145 \mu\text{m}$ and allows to measure objects not accessible to one-wavelength interferometers, i.e. surfaces with steps larger than half the optical wavelengths. Also, a temporary loss of the signals, e.g. due to poor reflecting parts of the surface, only leads to missing data for these areas and does not interrupt the scan as it would be the case for a fringe counting method.

Although the interferometer itself has a resolution of about 4 nm and its expected uncertainty is of the order of 20 nm, the resulting overall accuracy is unfortunately limited by the mechanical translation stages used in the experiments to values up to 250 nm for scan lines longer than 4 mm.

The interferometer reaches its limits on rough surfaces. Such surfaces could be measured, although the interferometer signal amplitude fluctuated and dropped partially to 10% of the value on smooth areas. For a calculation of the roughness parameters fringe counting was applied to get equally spaced data without missing points. The roughness parameters derived from these values are in good agreement with the calibration values of the roughness standards.

4. Precise length measurements of prismatic bodies

For many industrial applications precise measurement of prismatic bodies, e.g. gauge blocks, or cylindrical samples, by multi-wavelength interferometry is necessary for dissemination of the length unit metre, i.e. traceability of the length measurement. Precise length changes of such bodies with temperature (thermal expansion), pressure (compressibility), and time (long term stability) can be measured with PTB's Precision Interferometer. Figure 5 shows the interferometer situated in a temperature controlled and vacuum tight environmental chamber. The light provided by the three different lasers alternatively passes a fibre representing the entrance of the interferometer. The reference path of the interferometer can be varied for phase stepping by slightly tilting the compensation plate. The tilt angle is monitored by an auxiliary interferometer and servo controlled. For measurements in air the measuring path contains a 400 mm vacuum cell close to the sample to determine the refractive index of air at the specific environmental conditions.

A 512 x 512 pixel camera system (Photometrics CH 350) provides data frames at 16-bit per

pixel. Phase stepping interferometry based on intensity frames at 8 different phase steps is used to obtain the phase map of the sample including the end plate [12]. The centre position of the samples front faces with respect to the camera pixel coordinates is assigned [13]. Interferometer autocollimation was adjusted by retroreflection scanning before a measurement was started [14]. Three stabilised lasers are used subsequently in the measurements. The gauge block lengths resulting from using the two J₂-stabilised lasers at 532 nm and 633 nm were averaged. The Rb-stabilised laser at 780 nm is used for a coincidence check, only.

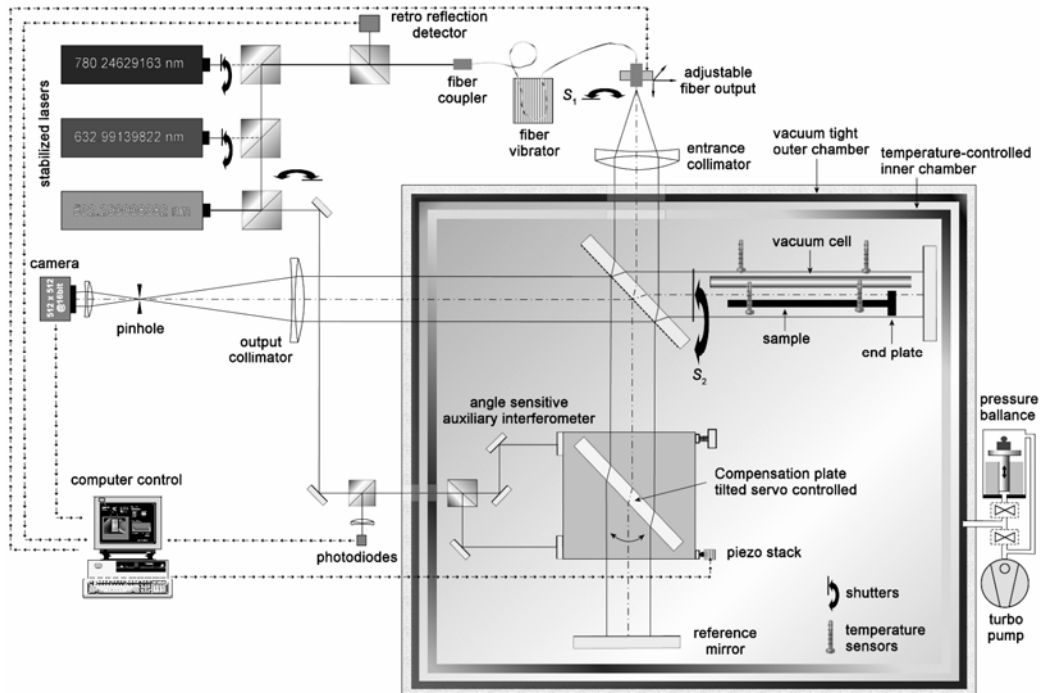


Fig. 5. Scheme of PTB's Precision Interferometer

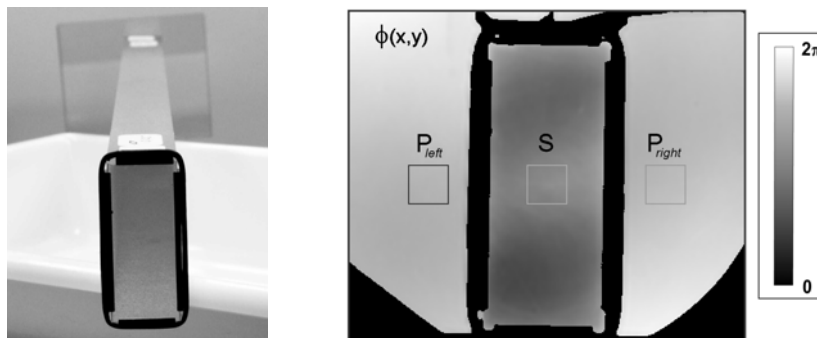


Fig. 6. Left: front view of the sample wrung to the end plate, right: measured interferogram with a region of interest (ROI) at the sample's front face (S) and two symmetrically arranged ROIs at the end plate ($P_{left/right}$)

The fractional order of interference, f , can be extracted from the interferogram. Figure 6, left, shows a photograph of a typical sample. At the right side the measured interferogram of this sample is shown. The rectangles indicate the regions of interest (ROIs) in which the phase values are averaged. This leads to the values ϕ_S , ϕ_P^{left} , and ϕ_P^{right} from which the fractional order of interference is calculated:

$$f = \frac{1}{2\pi} \left[\frac{1}{2} (\phi_P^{left} + \phi_P^{right}) - \phi_S \right]. \quad (7)$$

Using optical interferometry, the length L of a sample body is expressed as a multiple of the light wavelength used. For one-wavelength interferometry the exact knowledge of the integer interference order (entailed with a precision mechanical pre-measurement) would be required before the exact length can be determined. The use of different wavelengths, however, results in independent length which should coincide. The expected coincidence is predicted by the uncertainties for the individual λ_k and f_k , respectively. A variation technique can be used for the extraction of the integer orders of interference known as “method of exact fractions”. Here integer variation numbers δ_k are introduced in the length evaluation:

$$L_k = \frac{1}{2} \lambda_k (i_k + \delta_k + f_k), \quad (8)$$

in which i_k is evaluated from the estimated length $i_k = L^{est} / \frac{1}{2} \lambda_k$. At a set of $\{\delta_1, \delta_2, \dots\}$ the mean length \bar{L} and the average deviation Δ are calculated according to:

$$\bar{L} = \frac{1}{r} \sum_{k=1}^r L_k, \quad \Delta = \frac{1}{r} \sum_{k=1}^r |\bar{L} - L_k|. \quad (9)$$

The amount of Δ can be used as a coincidence criteria and displayed vs. the related values of \bar{L} . Fig. 7 shows a measurements example for this approach, in which the estimate length of the sample is 299.15 mm. The measurements were performed under vacuum conditions using three wavelengths λ_k subsequently, each measurement resulting in the fractions as given in Table 2.

Table 2.

| λ_k / nm | $u(\lambda_k)/\lambda_k$ | f_k (in example) | $u(f_k)$ | $u(L_k)$ /nm (in example) |
|------------------|--------------------------|-----------------------|----------|------------------------------|
| 532.290008382 | 3e-12 | 0.0271 | 0.0003 | 0.08 |
| 632.99139822 | 2.5e-11 | 0.1723 | 0.0004 | 0.13 |
| 780.24629163 | 1e-9 | 0.6465 | 0.0006 | 0.38 |

Obviously, a large number of values exist below a level of $\Delta = 5$ nm. The x-values of these points are separated by some tenth of micrometer. Certain minima of Δ exist whose separation exceeds very large values of more than 0.6 mm. It is tempting to identify the minimum closest to L^{est} with the length of the sample. However, before such conclusion, it is necessary to review the uncertainty of the length caused by the uncertainties of the individual wavelengths and fractional orders of interference. From (8) follows:

$$u(L_k)^2 = \left(L^{est} u(\lambda_k) / \lambda_k \right)^2 + \left(\frac{1}{2} \lambda_k u(f_k) \right)^2 \quad (10)$$

and, in case of the mentioned example with PTB's Precision Interferometer, the uncertainties $u(L_k)$ are close to 0.1 nm as depicted in the last column in Table 2.

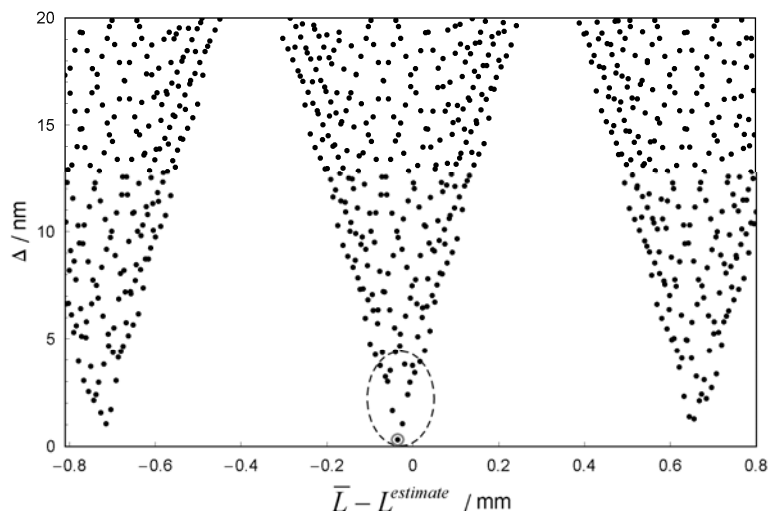


Fig. 7 The average length resulting from variations of the integer orders (x-coordinates of the data points) and the related average deviation.

The actual minimum, Δ_{\min} , is about 0.3 nm (see the data point marked by the grey circle in Fig. 7). This value is somewhat larger than the total uncertainty of the mean length, $u(\bar{L})$, resulting to 0.14 nm. The reason for this somewhat larger value of Δ_{\min} compared to 0.14 nm can be attributed to small constant influences onto the coincidence between the different lengths L_k as discussed in [15]. The low value of $u(\bar{L})$ together with the fact that the neighbouring points are off by more than 1 nm (see data points within the dashed circle of Fig. 7) justifies the conclusion that the mean length for which Δ_{\min} is found can be looked upon the actual length. Thus, the range of unambiguity is in fact about 0.6 mm as assumed in the above example. Therefore, a rough estimate of the length, obtained from a simple measurement, is sufficient for measurements at PTB's Precision Interferometer.

5. Conclusions

The multi-wavelength measurement technique is a proper method to remove ambiguity in interferometric length measurements. In general, the more accurate the fractions of the fringes can be measured, the larger is the range of unambiguity.

Based on this principle, an absolute distance interferometer has been developed for the measurement of long distances of up to approx. 10 m by combination of frequency-sweeping interferometry and two-wavelength interferometry, using two external cavity diode lasers. A comparison of the absolute distance interferometer to a counting HeNe laser interferometer shows a deviation below $0.5 \mu\text{m} + 0.5 \mu\text{m/m}$.

Furthermore, a three-wavelength diode laser interferometer has been developed for the measurement of surface profiles. An uncertainty of approx. 20 nm was achieved for a measuring range below 150 μm .

Finally, the example of PTB's Precision Interferometer demonstrates the benefit of three-wavelength interferometry. The length of bodies with parallel end faces (e.g. gauge blocks) can be measured there with an uncertainty of the averaged length below 0.3 nm, while the range of unambiguity is drastically enlarged. Therefore, an ultra precise length measurement at PTB's Precision Interferometer requires only a rough estimate of the length in advance.

Acknowledgements

The authors are grateful to the Deutsche Forschungsgemeinschaft (DFG) for financial support.

References

- [1] Abou-Zeid A. Diode Lasers for Interferometry, *J. of Prec. Eng.*, 11(3), 139, 1988.
- [2] Bodermann B, Burgarth V, and Abou-Zeid A. Modulation-free stabilised diode laser for interferometry using Doppler-reduced Rb transitions. In Proc. 2nd Euspen Topical Conf. (Turin), vol 1, ed A Balsamo et al, 2001, 294–297
- [3] Zarka A, Abou-Zeid A, et al. Intern. Comparison of Eight Semiconductor Lasers Stabilised on 127I2 at 633 nm, *Metrologia*, 37 (4), 329, 2000.
- [4] Bourdet GL and Orszag AG. Absolute distance measurements by CO2 laser multiwavelength interferometry, *Appl. Opt.* 18, 225–227, 1979.
- [5] Bechstein KH and Fuchs W. Absolute interferometric distance measurements applying a variable synthetic wavelength, *J. Opt.* 29, 179–182, 1998.
- [6] Kinder T and Salewski KD. Absolute distance interferometer with grating stabilised tunable diode laser at 633 nm, *J. Opt. A: Pure Appl. Opt.* 4, 364–368, 2002.
- [7] Hartmann L, Meiners-Hagen K, and Abou-Zeid A. An absolute distance interferometer with two external cavity diode lasers, *Meas. Sci. Technol.* 19, 045307 (6pp), 2008.
- [8] Bönsch G and Potulski E. Measurement of the refractive index of air and comparison with modified Edlens formulae, *Metrologia* 35, 133–139, 1998.
- [9] Heydemann PLM. Determination and correction of quadrature fringe measurement errors in interferometers, *Appl. Opt.* 20, 3382–3384, 1981.
- [10] Meiners-Hagen K, Burgarth V, and Abou-Zeid, A. Profilometry with a multi-wavelength diode laser interferometer, *Meas. Sci. Technol.* 15, 741–746, 2004.
- [11] Abou-Zeid A, Wolf M. Profilometry: using a diode laser interferometer with three wavelengths. In Proc. of the 1st euspen Topical Conf. on Fabrication and Metrology in Nanotechnology, Copenhagen, Denmark, L. De Chiffre and K. Carneiro (Eds.). Vol. 1, p. 137–140, 2004.
- [12] Schödel R, Nicolaus A, Bönsch G. Phase stepping interferometry: Methods to reduce errors caused by camera nonlinearities, *Appl. Opt.* 41, 55-63, (2002).
- [13] Schödel R, Decker JE. Methods to recognize the sample position for most precise interferometric length measurements, In Proc. SPIE, Vol. 5532, 237-247, 2004.
- [14] Schödel R, Bönsch G. Highest accuracy interferometer alignment by retroreflection scanning, *Appl. Opt.* 43, 5738-5743, 2004.
- [15] Schödel R, Nicolaus A, and Bönsch G. Minimizing interferometer misalignment errors for measurement of sub-nanometer length changes. In Proc. SPIE 2003, Vol. 5190, p. 34-42, 2003.